



Non-conventional synthesis and processing in the front-end of the nuclear fuel cycle

Nekonvenční syntéza a zpracování v počátku
jaderně-palivového cyklu

Habilitation thesis

Habilitační práce

Václav Tyrpekl

Praha, 2023

Foreword

Presented habilitation thesis stems from eighteen publications published in the years 2015-2022. All are focused on the frontend of the nuclear fuel cycle, both industrial and research fuels. Specifically, the work concerns precipitation techniques, which bring dissolved actinide salts (U^{4+} , Th^{4+} , U^{6+}) from solutions into solid powder, mostly oxides. Later, the powder are to be compacted and densified typically into fuel pellets, known from industrial power reactors. Apart from classical sintering by appropriate calcination cycle, this thesis describes the attempts to densify powders by so-called electrical field assisted sintering techniques, in particular spark plasma sintering. These techniques were developed very recently and some of the presented works present pioneering results in this field.

I would like to acknowledge colleagues and students, who greatly contributed to all the work discussed here. The list is not definitely complete; therefore, I would like to thank virtually to all, also those unfortunately not listed. Many thanks to my colleagues from JRC Karlsruhe, Germany: J-F. Vigier, M. Cologna, J. Somers, M. Holzhäuser D. Salvato; to colleagues from SCK·CEN, Belgium: T. Wangle, M. Verwerft, Ch. Schreinemachers. K. Vanaken. P. Dries., R. Lomelen. Additionally, I am much obliged to my colleagues and students from the Department of inorganic chemistry, Faculty of science, Charles University, in memoriam to Daniel Nižňanský, without him this work would not exist.

Lastly, big “thank you” belongs to my family and friends.

Table of contents

1	Introduction.....	4
1.1	Conventional frontend of UO_2 and ThO_2	8
1.2	Electrical field assisted sintering	9
2	Discussion of selected research	15
2.1	UO_2 , ThO_2 , UC, doped UO_2 powder preparation.....	16
2.2	Oxalate derived ThO_2 powder and its sintering performance	19
2.3	Application of oxalate derived oxide powders/pellets	21
2.4	Scrap recycling in ThO_2 pellets production	23
2.5	Spark plasma sintering of UO_2 , ThO_2 , UC powders	24
3	Conclusion	29
4	List of publications.....	31

1 Introduction

The first civil power reactor providing electricity was connected to the grid in Obninsk near Moscow (former USSR), supplying 5 MWe¹ on 27 June 1954². This success immediately triggered efforts in the construction of civil power reactors around the world. Soon, a carbon dioxide-cooled reactor of 5 MWe was commissioned in Marcoule, France in September 1956 and a 55 Mwe reactor in Calder Hall, UK in October 1956. The 1960's can be considered as a “genesis” of the nuclear power industry having about 4025 MWt of total power installed in the UK, 1528 MWt in France and 3077 MWt in the USA in 1969². Ever since, nuclear fission has been used for electricity and heat production to a degree depending on national traditions, the degree of engineering development, and especially on political will. In 2021 about 32 countries had a civil nuclear program, which contributed to national electricity production, see Figure 1.

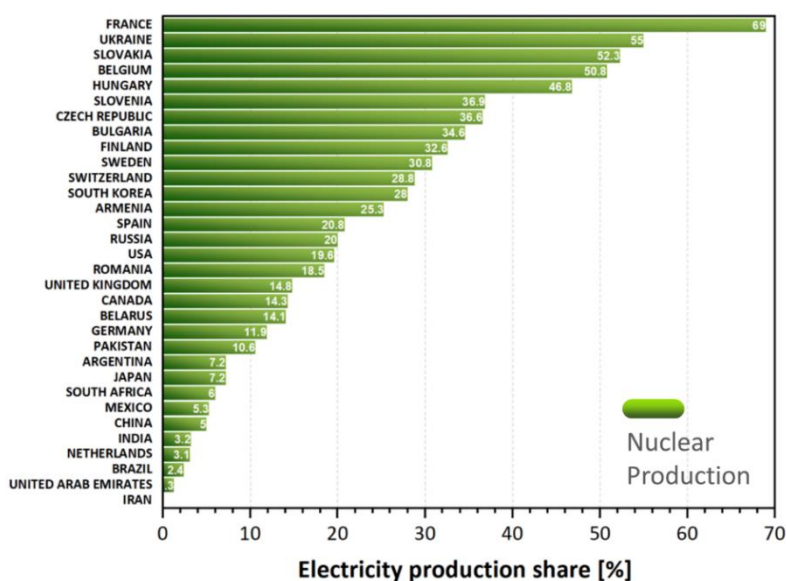


Figure 1 List of countries with active nuclear power industry and their electricity production share in 2021 (data from ref.³).

In a closer look at selected countries (Figure 2), the USA produced the largest total amount of electricity by nuclear production in 2021. However, the highest production share appertains traditionally to France. The Czech Republic belongs to countries with a strong tradition in the nuclear industry, not only from the viewpoint of the utility – currently running 6 power

¹ MW(e) – stands for MW electrical watts, MW(t) – stands for thermal watts.

² A.M. Petros'yants: A pioneer of nuclear power, IAEA Bulletin 26(4) (1984) 42-46.

³ International Atomic Energy Agency (IAEA), www.iaea.org, 21st July 2022.

reactors, but also from the viewpoints of nuclear power plant construction (steel industry experience) and research. The Czech nuclear fleet covers 4 pressurised water reactors (PWR, light water moderated and cooled) type VVER V-213 with a gross capacity of 510 MWe, all at the Dukovany site, and two PWR units VVER V-320 with 1055 MWe per unit at the Temelín site⁴. Altogether, the installed power represented 36.6 % of electricity production in the Czech Republic in 2021⁵.

The core of every technology producing energy is the fuel, e.g., hydrogen in a fuel cell, gasoil in a car engine, methane in a natural gas burner. In an active zone of a nuclear reactor, the type of fuel (composition, state of matter, design) depends on the technology used or foreseen. The prevalent PWR type of reactor employs uranium dioxide (UO₂, UOX, fluorite type) or mixed uranium-plutonium dioxide fuel (U_xPu_{1-x}O₂, MOX, fluorite type)⁵. New concepts of reactors, typically fast neutron reactors, might use actinide carbides, nitrides, silicides, molten salts, or other materials. These fuel types are currently under research and are used quite sporadically at the moment.

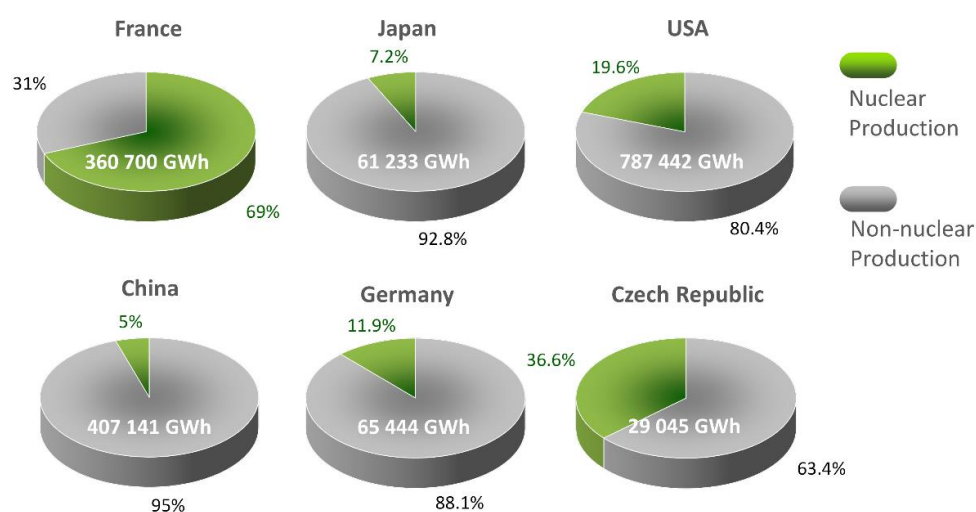


Figure 2 Electricity production share of selected countries in 2021, nuclear production (green), non-nuclear production (grey), and total electricity production in GWh by each nuclear sector (in white)⁶.

In contrast, oxide fuel fabrication, irradiation, and reprocessing have reached an advanced level of knowledge and engineering in the past years. The fuel lifetime is generally called the

⁴ <https://www.cez.cz/cs/o-cez/vyrobnizdroje/jaderna-energetika/jaderna-energetika-v-ceske-republice>, 21st July 2022

⁵ T. Abe, K Asakura: Uranium oxide and MOX production, chapter 2.15 in Comprehensive Nuclear Materials, Elsevier, 2012.

⁶ International Atomic Energy Agency (IAEA), www.iaea.org, 21st July 2022.

“nuclear fuel cycle”. However, this plain phrase comprises several meanings⁷:

- *Open fuel cycle* – Not a real cycle. The spent fuel is considered as a waste, and it is stored, for example, in a deep-ground repository. This is the case of the current Czech national strategy⁸.
- *Reprocessing fuel cycle* – Typically, uranium and plutonium (and possibly other minor actinides) are chemically extracted from spent fuel and reused for fresh MOX fuel fabrication.
- *Breeding cycle* – The spent fuel of a fast breeder reactor contains more fissile material than fresh fuel. In this reprocessing cycle, this fissile material (plutonium) can be extracted and reused analogically, as in the previous cases.

A simplified sketch of the reprocessing nuclear fuel cycle, applied, for example, in France, is shown in Figure 3. Additionally, the nuclear fuel cycle can be divided into two main areas depending on its irradiation state (before or after removal from the reactor)⁷:

Front-end – it covers the following topics: i) Uranium ore mining, milling, and conversion to UF₆; ii) Isotopic enrichment; iii) conversion to UO₂, powder pressing, and sintering; iv) Fuel elements fabrication. The front-end covers quality control of produced pellets and reuse of the production scrap back into the second step, so no waste remains. Additionally, the lifetime of the fuel inside the active zone connected with irradiation, fission, and build-up reactions can be considered as the fuel cycle front-end.

Back-end – After appropriate cooling, the irradiated fuel can be stored in interim or final disposals. Another possibility is to reprocess the fuel with the aim of uranium and plutonium recovery for further use. The PUREX process (recovery of U and Pu) has been industrially applied since 2004⁹. Many advanced reprocessing routes are under investigation, for example, minor actinides extensions of PUREX, DIAMEX^{9,10} focused on the recovery of trivalent actinides

⁷ D. Bodansky, Nuclear Energy: Principles, Practices and Prospects, 2nd edition, Springer, 2004

⁸ <https://www.sujb.cz/jaderna-bezpecnost/nakladani-s-vyhorelym-jadernym-palivem>, 21st July 2022

⁹ J-P. Glatz: Spent fuel dissolution and reprocessing processes, chapter 5.14 in Comprehensive Nuclear Materials, Elsevier, 2012.

¹⁰ L. Nigond, C. Musikas, C. Cuilerdier: Extraction by N,N,N',N-tetraalkyl-2alkylpropane-1,3diamides. I. H₂O, HNO₃ and HClO₄, Solvent Extraction and Ion Exchange 12(2) (1994) 261-269.

using diamides, or non-aqueous route using molten salts called pyroprocessing¹¹, etc.

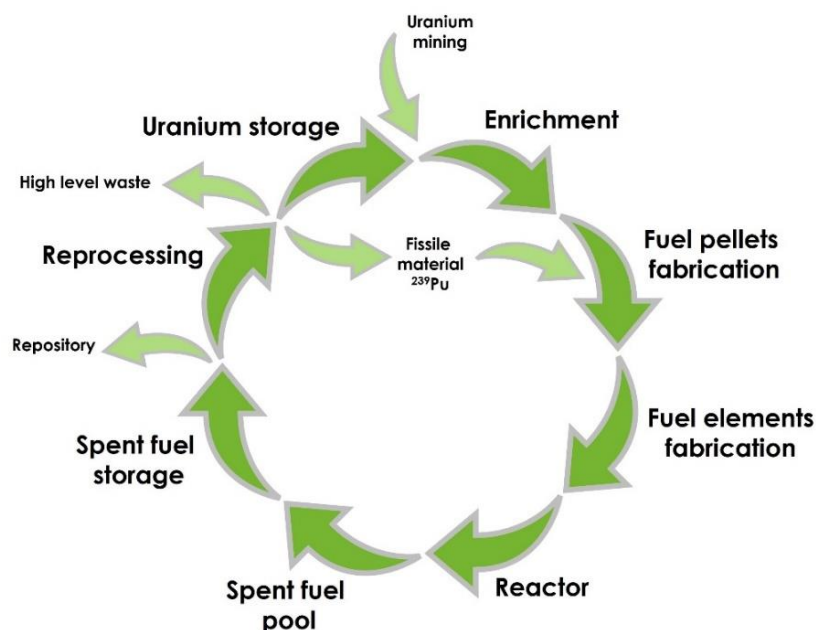


Figure 3 Simplified sketch of the nuclear fuel cycle (inspired by Figure 1 in ref.⁹).

In addition to the currently industrially applied uranium-based nuclear fuel cycle, this thesis concerns the thorium-based nuclear fuel cycle^{12,13}. It is less developed and commercially applied than the uranium-based one. However, it includes many benefits, which makes it attractive for future concepts. Thorium is more abundant in the Earth's crust than uranium and is almost monoisotopic. ^{232}Th is not a fissile isotope for thermal neutrons but yields fissile ^{233}U with a high conversion factor. A great advantage is that the ^{232}Th - ^{233}U system can work with fast, epithermal, or thermal neutrons. Besides the molten salt reactor concept¹⁴, the thorium fuel is also considered as oxide (ThOX or MOX). However, thorium dioxide (fluorite) is an extremely stable material with the highest melting point of all oxides¹⁵, which makes its processing (sintering, dissolution) challenging and energy demanding.

¹¹ E-Y. Choi, S. M. Jeong: Electrochemical processing of spent nuclear fuels: An overview of oxide reduction in pyroprocessing technology, *Progress in Natural Science: Materials International* 25(6) (2015) 572-582.

¹² Thorium fuel cycle – Potential benefits and challenges, International Atomic Energy Agency, IAEA-TECDOC-1450, 2005.

¹³ D. Haas, M. Hugon, M. Verwerft, Overview of European experience with thorium fuels, Chapter 18, in *Nuclear back-end and transmutation technology for waste disposal*, Springer, 2015.

¹⁴ J. Serp, M. Allibert, O. Beneš, S. Delpéch, O. Feynberg, V. Ghetta, D. Heuer, D. Holcomb, V. Ignatiev, J.L. Kloosterman, L. Luzzi, E. Merle-Lucotte, J. Uhlíř, R. Yoshioka, D. Zhimin: The molten salt reactor (MSR) in generation IV: Overview and perspectives, *Progress in Nuclear Energy* 77 (2014) 308-319.

¹⁵ T.R. Pavlov, T. Wangle, M.R. Wenman, V. Tyrpekl, L. Vlahovic, D. Robba, P. Van Uffelen, R. Konings, R.W. Grimes: High temperature measurements and condensed matter analysis of the thermo-physical properties of ThO_2 , *Scientific Reports*, 8 (2018) 5038.

1.1 Conventional frontend of UO_2 and ThO_2

Uranium-containing fuel has been predominant since the early years of nuclear energy application for electricity generation. Although nuclear fuel is not generally considered as fossil fuel, uranium ore must be mined and then mechanically and chemically processed. The world production of U has oscillated around 50 kt of U metal per year in the past decades. Currently, the biggest producers of uranium ore are Canada, Kazakhstan, Australia, and Namibia, covering about half of the total annual production, which was approximately 48.5 kt of U in 2021¹⁶. Uranium ore processing yields so-called yellow cake, which is converted through UO_2 powder to UF_6 for ^{235}U enrichment (3-5%). Three main industrial pathways of conversion to UO_2 exist at the moment¹⁷: i) the Ammonium diuranate reconversion process, ii) the Ammonium uranium carbonate reconversion process, and iii) the Integrated dry route. All routes give powders of UO_{2+x} with different characteristics (oxygen/metal ratio, specific surface area, grain size, etc.) and minor contaminant concentrations (e.g., fluorine, carbon). The subsequent processing (actual fuel pellet fabrication) is schematically depicted in Figure 4. An important fact is that the production process is basically waste-free since all the production waste (scrap pellets, powder after pellet grinding, etc.) is oxidized to U_3O_8 and reused as a sintering additive. Pressed pellets are typically sintered in a continuous furnace at 1600-1700 °C to 95% of theoretical density. A pellet of adequate quality is free of large cracks and porosities, and the edges are chamfered. The pellet's bases show a convex spherical profile, a so-called dish, for better stability during the lifetime in a reactor. Reactor pins, typically with Zr-alloy claddings, are put into assemblies, which are loaded into the reactor's active zone. Recent numbers of UO_2 pellets production are not easily accessible in open texts. However, to give an impression, the flyer of FBFC S.A. (Framatom, Franco-Belge de Fabrication de Combustible) from 1999 estimates the number of pellets produced on six production lines to be more than 230 000 000 per year¹⁸.

Contrariwise to uranium, thorium is produced mainly as a side product of lanthanides extraction from monazite sands/deposits¹⁹. Wangle reviewed the attempts to produce

¹⁶ World Nuclear Association, Uranium mining overview 2021

¹⁷ Nuclear Fuel Cycle Information System, International Atomic Energy Agency, IAEA-TECDOC-1613, 2009.

¹⁸ FBFC, Framatome: De l'usine au cœur du réacteur, 31-15, Paris, 1999

¹⁹ V.S. Keni, Extraction and refining of thorium, Proceedings of the Indo-Japan seminar on thorium utilization Indian Nuclear Society, Bombay, India, December 10-13, 1991.

thorium fuel cycle on an industrial level, namely powder production and sintering into fuel pellets²⁰. In the past, there has been no real industrialisation of the thorium dioxide fuel cycle. Few attempts were made on large-scale fuel production for research reactors (e.g., ²³⁵U-²³²Th oxide fuel for Borax IV reactor²¹). Most of the ThO₂ powder production has been based on oxalate precipitation and calcination. The ThOX fuel pellet production process will follow similar powder pressing steps as UO₂. But, as mentioned earlier, the sintering to full density requires higher temperatures (1700-1800 °C) under air, which is at the very limit of classical corundum/superkanthal furnace technology.

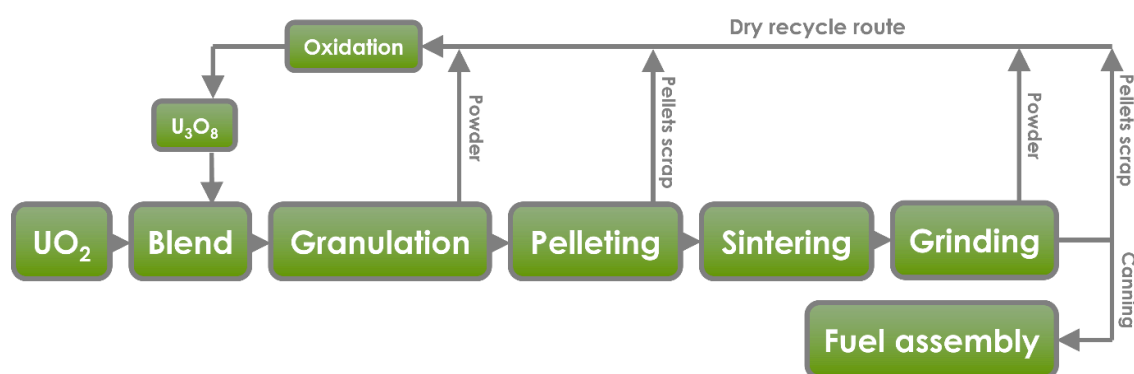


Figure 4 Simplified flowchart of UO₂ industrial fuel production emphasizing the waste free approach (inspired by Figure 12 in ref.²²).

1.2 Electrical field assisted sintering

The process of ceramics sintering is almost as old as civilisation itself. It is mainly known for production of ceramics and porcelain for daily use. As mentioned above, sintering is an important part of nuclear fuel production, not only for industrial but also for research fuel. During sintering, the powder compact goes through a heating cycle, which ensures densification (compaction) and grain growth. The final sintering product should show a considerable degree of densification, mechanical integrity, endurance, toughness, and hardness. Nowadays, various sintering techniques exist. The oldest and most basic sintering approach considers powder shaping and applying an adequate heating cycle. The densification (density change in time) can be described by the model expressed in Equation 1, part denoted

²⁰ T. Wangle, Improving the sintering behaviour of thorium oxide, Doctoral thesis, KU Leuven, Belgium, 2020.

²¹ D.K. Walker, R.A. Noland, F D. McCusig, C.C. Stone: Borax-IV reactor: Manufacture of fuel and blanket elements, Argonne National Laboratory, ANL-5721, 1958.

²² Minimization of waste from uranium purification, enrichment and fuel fabrication, International Atomic Energy Agency, IAEA-TECDOC-1115, 1999.

A²³. A more recent technique uses external pressure applied on the sample during calcination. Apart from the heat effect, the pressure should contribute significantly to the densification mechanism, for example, by particle fragmentation and rearrangement, deformation of zones of contacts, shrinkage of individual pores, and creep²⁴. Part B in Equation 1 represents the function of external pressure. Since more models exist, the function is expressed generally. Recent investigations revealed that electrical field/current can increase the efficiency of the densification process in addition to heat and pressure^{25,26}. The exact physical model that would describe part C of Equation 1 is currently unavailable, but several phenomena have been identified already, e.g., Joule heating, defects creation, diffusion driving force, and electromigration. In general, the simplified description of all different aspects of sintering is covered in Equation 1,

$$\frac{d\rho}{dt} = \underbrace{\left(\frac{3\rho\gamma\Omega\Gamma}{kTG^n} D_0 e^{-\frac{Q}{RT}}\right)}_A \cdot \underbrace{f(P_{ext})}_B \cdot \underbrace{f(U, I)}_C \quad \text{Eq. 1}$$

where ρ stands for density, γ is surface energy, Ω is atomic/ionic volume, Γ is a parameter related to the driving mechanism (diffusion distance, geometric features, linear shrinkage), k is the Boltzmann constant, R gas constant, D diffusion coefficient, G grain size, and Q is the activation energy of sintering. The exponent n relates to the sintering mechanism.

Electrical field-assisted sintering (FAST) represents a modern and growing discipline of material processing. The very first footmarks can be found in 1906 when Lux used Joule heating to sinter tungsten and molybdenum wires²⁷. Shortly after, Weintraub and Rush showed that resistance sintering at elevated temperatures could be used to produce monoliths from materials with low or zero electrical conductivity²⁸. The FAST technology has made a significant step forward since then. In the 1960s, Inoue laid the foundations of the

²³ H. Su, D.L. Johnson: Master sintering curve: A practical approach to sintering, *Journal of American Ceramic Society* 79 (1996) 3211-3217.

²⁴ E. Artz: Hot isostatic pressing: Developments in theory, *Concise Encyclopedia of Advanced Ceramic Materials*, 215-219, Elsevier, 1991.

²⁵ O. Guillon, J. Gonzalez-Julian, B. Dargatz, T. Kessel, G. Schierner, J. Rthel, M. Herman: Field-assisted sintering technology/Spark plasma sintering: Mechanisms, materials, and technology developments, *Advances Engineering Materials* 16 (2014) 830-849.

²⁶ M. Biesuz, V.M. Sglavo: Flash sintering of ceramics, *Journal of European Ceramic Society* 39 (2019) 115-143.

²⁷ Lux J., patents: CH 35994 (1906), DK 8621 (1906), FR 374543 (1907); Bloxam A. G. (Lux J.): GB 9020 (1906), GB 27,002 (1906).

²⁸ G. Weintraub, H. Rush: US patent 1071488A, 1912.

most common FAST technique called “Spark Plasma Sintering” (SPS) by using graphite punches/die setup and DC pulsed electric current²⁹. The profound research and technological expansion of SPS came in early 2000, for all the works of Munir et al.³⁰ or Vanmeensel et al.³¹ Typically, SPS uses graphite punch/die setup, DC pulsed current, applied pressure up to 100 MPa, voltage up to 10 V and current of several kA. The temperature during such process can reach 2200 °C. In 2010 Cologna et al.³² described fast (<5 s) sintering of nanograin zirconia at 850 °C using electrical fields up to 120 V/cm. This and other works of Cologna et al.^{33,34} opened a new field of the FAST branch called flash sintering (FS). Afterward, the flash sintering patent came in 2015 by Raj³⁵. As previously mentioned, FS uses higher electrical fields than SPS, and it is characterised by a so-called “flash event”, a moment of rapid compaction, temperature increase by Joule heating, decrease of resistivity and luminescence²⁶. This is typically seen for ionic conductors (e.g., yttria-stabilized zirconia) with non-linear evolution of the electrical conductivity with temperature. In time, several versions of FAST techniques or their combinations have gained popularity in the research community³⁶. Apart from the most common SPS (Figure 5A), it is the high-pressure version of SPS, which typically uses silicon carbide punches (Figure 5B), flash sintering, and flash sintering in SPS configuration with applied external pressure (Figure 5C and D).

M. Cologna reviewed the application of FAST techniques in nuclear ceramics manufacturing³⁷. Apart from a few very first publications in the early 2000s, the main increase in published

²⁹ Inoue K., patents: US 3,241,956 (1966), US 3,250,892 (1966), US 3,340,052 (1967).

³⁰ Z.A. Munir, U. Anselmi-Tamburini, M. Ohyanagi: The effect of electric field and pressure on the synthesis and consolidation of materials: A review of the spark plasma sintering method, *Journal of Materials Science* 41 (2006) 763-777.

³¹ K. Vanmeensel, A. Laptev, J. Hennicke, J. Vleugels, O. Van Der Biest: Modelling of the temperature distribution during field assisted sintering, *Acta Materialia* 53 (2005) 4379-4388.

³² M. Cologna, B. Rashkova, R. Raj: Flash sintering of nanograin zirconia in < 5 s at 850 C, *Journal of the American Ceramic Society* 93 (2010) 3556-3559.

³³ M. Cologna, J.S.C. Francis, R. Raj: Field assisted and flash sintering of alumina and its relationship to conductivity and MgO-doping, *Journal of the European Ceramic Society* 31 (2011) 2827-2837.

³⁴ R. Raj, M. Cologna, J.S.C. Francis: Influence of externally imposed and internally generated electrical fields on grain growth, diffusional creep, sintering and related phenomena in ceramics, *Journal of the American Ceramic Society* 94 (2011) 1941-1965.

³⁵ R. Raj, M. Cologna, A.L. Geromal Prette, V.M. Sglavo, J.S.C. Francis: US 8,940,220 B2 (2015).

³⁶ T. Wangle, M. Vilémová, V. Tyrpekl: Methods of Electrical Field/Current Assisted Sintering, *Chemické Listy* 166 (2022) 343-347.

³⁷ M. Cologna: Use of Field Assisted Sintering for Innovation in Nuclear Ceramics Manufacturing, Chapter 5.25 in *Comprehensive Nuclear Materials* (2nd Edition), Elsevier, 2020.

research came ten years later. The first study by Ge et al.³⁸ from the University of Florida (UF), Gainesville, describing the compaction of UO_2 pellets by SPS dates to 2013. The efforts in the nuclear fuel R&D using FAST techniques became evident at several research institutes:

i) University of Florida, Gainesville, U.S.A.; ii) Royal Institute of Technology (KTH), Stockholm, Sweden; iii) Joint Research Centre (JRC), Karlsruhe, Germany, where most of the early works are part of the presented thesis. The very first publication coming from UF on UO_2 ³⁸ described the systematic variations of spark plasma sintering parameters. It was shown that a maximal temperature of 1050 °C with a dwell time of only 30s gave pellets with a theoretical density of 96% while maintaining adequate mechanical properties.

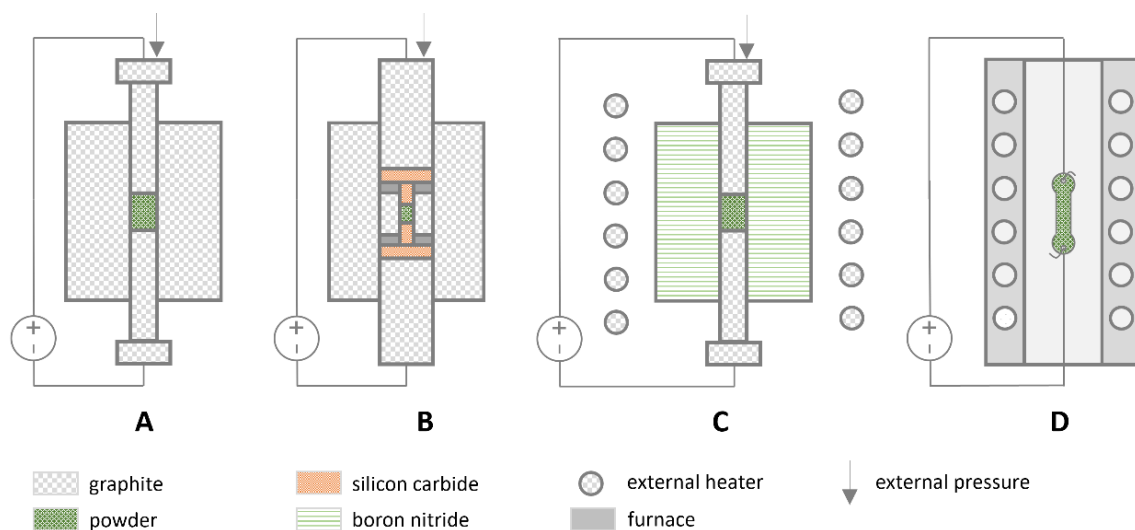


Figure 5 Simplified sketches of the most popular FAST techniques in the research community (inspired by Fig. 1 in ref³⁶).

Later, the same group published a work describing the thermal conductivity measurements of UO_2 pellets prepared by SPS using various conditions³⁹. In this work, the authors, for the first time, mentioned the reduction of oxygen-overstoichiometric UO_{2+x} to $\text{UO}_{2.00}$ by the SPS process. Shortly on this, it is in the nature of UO_2 powders to gain oxygen from the atmosphere and form UO_{2+x} . Uranium, a large actinide element, has three valence states +IV, +V, +VI, and a significant tendency to form non-stoichiometric compounds. Such behaviour can be

³⁸ L. Ge, G. Subhash, R.H. Baney, J.S. Tulenko, E. McKenna: Densification of uranium dioxide fuel pellets prepared by spark plasma sintering (SPS), *Journal of Nuclear Materials* 435 (2013) 1-9.

³⁹ L. Ge, G. Subhash, R.H. Baney, J.S. Tulenko: Influence of processing parameters on thermal conductivity of uranium dioxide pellets prepared by spark plasma sintering, *Journal of Nuclear Materials* 34 (2014) 1791-1801.

described by the U-O phase diagram⁴⁰ and was reviewed by Leinders⁴¹. The highly reductive SPS environment (graphite tooling, electric current) led to a partial reduction of UO_{2+x} and, at certain conditions even to $\text{UO}_{2.00}$. Further, the UF team studied the upgrading of the thermal and mechanical properties of UO_2 by SPS co-sintering with diamond⁴², carbon nanotubes⁴³, or silicon carbide⁴⁴. Additionally, the team performed a first study to explore the possibility of the commercial fabrication of nuclear fuel by SPS⁴⁵. The authors conducted a set of tests for single and multiple-fuel pellet manufacturing. The final pellets were qualified against the commercial nuclear fuel, while all the demands were met except the grain size. Also, the main factor affecting the industrialisation of SPS is the degradation of commonly used graphite tooling.

The early works at KTH described the densification of uranium nitride⁴⁶. Uranium nitrides and carbides are typically tricky to sinter to high density by classical sintering (heating cycle at 1500-1750 °C)⁴⁷, however, SPS technology allowed to sinter UN to 99.8% density at 1650 °C with 3 minutes dwell time and 134 MPa of applied pressure. Later, the KTH team published a work describing the SPS fabrication of UN- U_3Si_2 composites aiming at accident-tolerant fuel applications⁴⁸. This work revealed new information about the ternary system U-Si-N and showed the possibility of producing high-density composites. Moving further, pure and Mo-doped U_3Si_2 was sintered using SPS⁴⁹. Pellets with high density (>95%) can be obtained by SPS at 1300 °C, while Mo had no solubility in the silicide phase below 1200 °C. The KTH team

⁴⁰ J.D. Higgs, B.J. Lewis, W.T. Thompson, Y. He: A conceptual model for the fuel oxidation of defective fuel, *Journal of Nuclear Materials* 366 (2007) 99-128.

⁴¹ G. Leinders: Low-temperature oxidation of fine UO_2 powders, Ph.D. thesis, KU Leuven, 2016.

⁴² Z.Chen, G. Subhash, J.S. Tulenko: Spark plasma sintering of diamond-reinforced uranium dioxide composite fuel pellets, *Nuclear Engineering and Design* 294 (2015) 52-59.

⁴³ A. Cartas, H. Wang, G. Subhash, R. Baney, J.S. Tulenko: Influence of carbon nanotube dispersion in UO_2 -Carbon nanotube ceramic matrix composites utilizing spark plasma sintering, *Nuclear Technology* 189 (2015) 258-267.

⁴⁴ Z. Chen, G. Subhash, J.S. Tulenko: Master sintering curves for UO_2 and UO_2 -SiC composite processed by spark plasma sintering, *Journal of Nuclear Materials* 454 (2014) 427-433.

⁴⁵ T. Ironman, J.S. Tulenko, G. Subhash: Exploration of viability of spark plasma sintering for commercial fabrication of nuclear fuel pellets, *Nuclear Technology* 200 (2017) 144-158.

⁴⁶ K. Johnson, J. Wallenius, M. Jolkkonen, A. Claisse: Spark plasma sintering and porosity studies of uranium nitride, *Journal of Nuclear Materials* 473 (2016) 13-17.

⁴⁷ A. Fernandez, J. McGinley, J. Somers, M. Walter: Overview of past and current activities on fuels for fast reactors at the Institute for Transuranium Elements, *Journal of Nuclear Materials* 392 (2009) 133-138.

⁴⁸ K.D. Johnson, A.M. Raftery, D.A. Lopez, J. Wallenius: Fabrication and microstructural analysis of UN- U_3Si_2 composites for accident tolerant fuel applications, *Journal of Nuclear Materials* 477 (2016) 18-23.

⁴⁹ D.A. Lopez, A. Benarosch, S. Middleburgh, K.D. Johnson: Spark plasma sintering and microstructural analysis of pure and Mo doped U_3Si_2 pellets, *Journal of Nuclear Materials* 496 (2017) 234-241.

afterward extended the works on UN by a grain growth study in SPS⁵⁰. The density and grain size was adjusted by controlling the pressure, temperature, and dwell time. Grains as large as 31 μm and densities up to 96% were obtained at 1650 °C for such material.

Lastly, the JRC Karlsruhe, which launched a SPS facility able to handle radioactive materials in late 2014 (see Figure 6), started to publish on the FAST sintering of nuclear fuel materials in 2015. The early research works done in this area are part of this thesis and will be described in the following chapters.

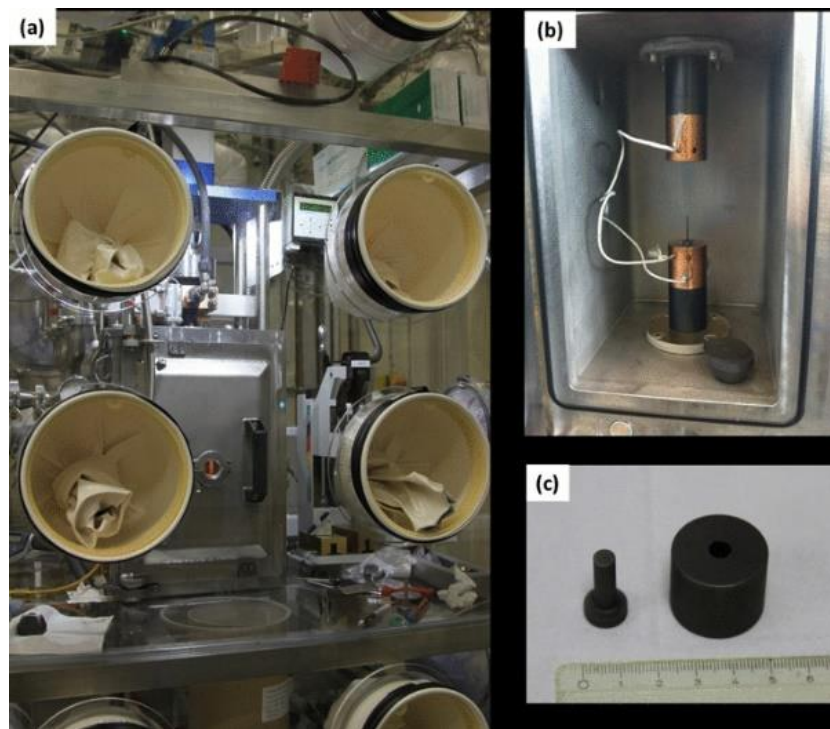


Figure 6 The SPS facility in JRC Karlsruhe, Germany (a), the sintering chamber (b), and the graphite punch/die set-up (taken from publication XII).

⁵⁰ K.D. Johnson, D.A. Lopez: Grain growth in uranium nitride prepared by spark plasma sintering, *Journal of Nuclear Materials* 503 (2018) 75-80.

2 Discussion of selected research

The presented thesis discusses research works dealing with the nonconventional front-end of the nuclear fuel cycle. As implied from the introduction, the following topics are included: powder preparation, powder pelletisation and sintering, recycling of pellet scrap, novel methods of sintering (FAST), and examples of research applications of selected products.

The word “nonconventional” should be explained in the context of the thesis. As mentioned in the introduction, conventional (industrial) nuclear fuel production uses particular processes and compounds (ammonium diuranate, uranium fluoride, etc.). Here, the main goal is to produce nuclear fuel for research purposes and describe certain important compounds' behaviour and nature. Since oxalic precipitation is industrially applied in the nuclear fuel cycle for the separation of plutonium and widely used in the technology of lanthanides and actinides⁵¹, significant attention is given to uranium and thorium oxalates, oxalate-derived nanocrystalline oxides, and their sintering behaviour. The applications of oxalic precipitation in the ThO₂ pellet scrap recycling route (based on triflic acid) is also discussed. Moreover, research applications of oxalate-derived oxides are shown in the case of physical properties measurements of ThO₂ (e.g., the highest melting point of all oxides) and production of fluorides for molten salt reactor applications. A large part is devoted to “nonconventional” sintering techniques of thorium and uranium oxides, oxalate derived oxide powders including. Most of the works describe the spark plasma sintering and high-pressure spark plasma sintering of actinide oxides aiming at the research fuel preparation, for example, mimicking the high burn-up structure⁵², spent fuel surrogates or for exploring the basic electrical field phenomena during FAST sintering. Most of the materials discussed below cannot be prepared by conventional sintering (application of pressure-less heating cycle), therefore, the application of the FAST technology for the sample preparation is a necessary step opening new research areas. Above all, the products allowed to conduct so-called separate effect tests, which are not possible to be carried out on the spent fuel due to price, high radiation, or by complexity. Lastly, the thesis touches on the nonconventional preparation and sintering of Gen IV fuels, namely uranium carbide.

⁵¹ F. Abraham, B. Arab-Chapelet, M. Rivenet, C. Tamain, S. Grandjean: Actinide oxalates, solid state structures and applications, *Coordination Chemistry Reviews* 266-267 (2014) 28-68.

⁵² V.V. Rondinella, T. Wiss: The high burn-up structure in nuclear fuel, *Materials Today* 13 (2010) 24-32.

2.1 UO₂, ThO₂, UC, doped UO₂ powder preparation

Oxalates are important salts in the technology of actinides⁵¹ and lanthanides⁵³. The main reason for the scientific and technological attention is their extremely low solubility in aqueous solutions. For example, the solubility product of Th(C₂O₄)₂·6H₂O is about 10⁻²⁵, which makes oxalate anoint efficient quantitative separation agent⁵⁴. Oxalates are low-cost, simple, and embody technologically desirable properties. They are crucial compounds in the separation and recovery of plutonium during fuel reprocessing on an industrial level⁵⁵. Another motivation to use oxalate precipitation instead of ammonia precipitation (hydrolysis) is to limit the amount of ammonium nitrate in the waste solutions and materials, and therefore preclude the possible explosion risk. **Publication I** described the preparation of (N₂H₅)₂U₂(C₂O₄)₅·nH₂O and Th(C₂O₄)₂·2H₂O and their thermal decomposition to nanocrystalline oxides. The crystallisation of ThO₂ and UO₂ from the oxalate precursors was in-situ monitored by high-temperature powder X-ray diffraction (PXRD) and thermogravimetry (TGA) and ex-situ by other techniques like Raman spectroscopy and electron microscopy (EM). Apart from the evolution of the grain size and linear thermal expansion coefficients of the nanocrystalline oxides, the purity of the products was examined. It was found that especially UO₂ when obtained by oxalate decomposition (conversion) under an argon atmosphere, contains considerable amounts of carbonates. The carbonate content (as released CO₂) was about 3.4 wt.% for the sample obtained at 600 °C and 1 hour dwell. With calcination temperature, the amount of carbonates decreased, for the sample obtained at 800 °C and 1 hour dwell, the content was only about 1 wt.%. It was demonstrated that oxalate precipitation and thermal conversion to oxide is a low-cost and robust technique for nanocrystalline UO₂ and ThO₂ preparation with desired grain size and purity.

This work was extended for thorium in **publication II**. It was found that by changing basic precipitation conditions (temperature, concentration, pH, strike⁵⁶), various morphotypes of

⁵³ C.N.R. Rao, S. Matarajan, R. Vaidhyanathan: Vaidhyanathan, R. Metal carboxylates with open architectures. *Angewante Chemie - International Edition* 43 (2004) 1466-1496.

⁵⁴ A.G. Kurnakova, L.K. Shubochkin: Solubility of Th(C₂O₄)₂·6H₂O in aqueous HNO₃ and H₂C₂O₄ at 25 °C. *Russian Journal of Inorganic Chemistry* 8 (1963) 647-650.

⁵⁵ R.M. Orr, H.E. Sims, R.J. Taylor: A review of plutonium oxalate decomposition reactions and effects of decomposition temperature on the surface area of the plutonium dioxide product, *Journal of Nuclear Materials* 465 (2015) 756-773.

⁵⁶ Both versions of precipitation were performed - "direct strike" (oxalic acid solution dropped into thorium solution, "DS") and "reverse strike" (thorium solution dropped into oxalic acid solution, "RS").

thorium oxalate can be obtained, see examples in Figure 7. One of the main disadvantages of oxalic precipitation is that the reaction is very prompt and, therefore, not easily controllable. However, more considerable changes in reaction conditions (logarithmic scale) can significantly affect the product morphology while saving the composition even at high solution acidity or temperature. The fast reaction kinetics was recently overcome by controlling the slow in-situ oxalic acid production in the metal salt solution by thermal decomposition of oxamic acid (monoamide of oxalic acid)⁵⁷. In other words, heterogeneous precipitation (mixing two solutions by dropping one to another) was replaced by homogeneous precipitation, where the precipitation agent is created inside the metal solution. This reaction can control then the precipitation kinetics and, for example, allow the growth of oxalate monocrystals. In general, homogeneous precipitation or homogeneous hydrolysis of metal ions are exciting and valuable methods that slow down the kinetics of precipitation/hydrolysis and allow to control of the homogeneity and morphology of the product^{58,59}. To complete, metal salt hydrolysis is usually done by pH increase of metal salt solution by addition of alkaline hydroxide solution (heterogeneous hydrolysis).

Urea (carbamide) is a top-rated precipitation agent for the homogeneous hydrolysis of metal ions in aqueous solutions⁶⁰. Upon heating to 100 °C, urea decomposes to carbon dioxide and ammonia, which leads to the gradual increase of pH and hydrolysis of metals yielding insoluble metal oxides/hydroxides.

Publication III describes the homogeneous hydrolysis of thorium by the thermal decomposition of urea and characterisation of the product. The starting solution was thorium nitrate in nitric acid with a pH equal to 1.5, urea was added in different molar ratios to the thorium solution and heated to 90 or 100 °C. The kinetics of pH evolution depended on the excess of urea, it is shown in Figure 8 (left). The typical hydrolysis plateau at pH = 4.5 was observed, during which milky blurring of the solution occurred, indicating the formation of

⁵⁷ A. Alemayehu, A. Zakharanka, V. Tyrpekl: Homogeneous precipitation of lanthanide oxalates, ACS Omega 7 (2022)

⁵⁸ V. Houšková, V. Štengl, S. Bakardjieva, N. Murafa, V. Tyrpekl: Photocatalytic properties of Ru-doped titania prepared by homogeneous hydrolysis, Central European Journal of Chemistry 7 (2009) 259-266.

⁵⁹ V. Tyrpekl, J.P. Vejpravová, A.G. Roca, N. Murafa, L. Szatmary, D. Nižňanský: Magnetically separable photocatalytic composite γ -Fe₂O₃@TiO₂ synthesized by heterogeneous precipitation, Applied Surface Science 257 (2011) 4844-4848.

⁶⁰ G.J.d.A.A. Soler-Illia, M. Jobbágy, A.E. Regazzoni, M.A. Blesa: Synthesis of nickel hydroxide by homogeneous alkalization. Precipitation mechanism, Chemistry of Materials 11 (1999) 3140-3146.

nanocrystalline ThO_2 (Figure 8 right). Radium, a daughter element of ^{232}Th , was also coprecipitated as carbonate from the solution to the solid phase. Gamma spectrometry revealed that about 80% of radium is coprecipitated in 24-hour experiments.

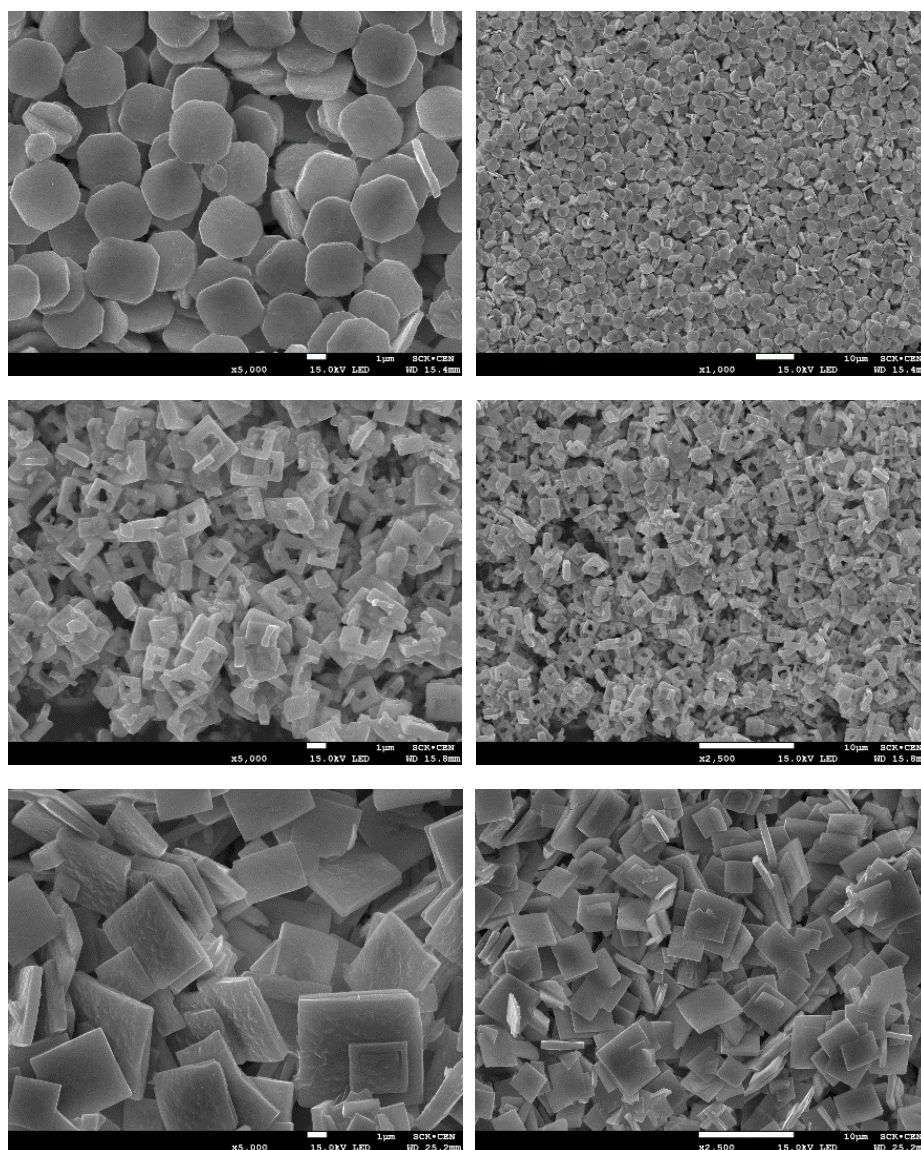


*Figure 7 Examples of thorium oxalate morphotypes obtained by precipitation using a low concentration of oxalic acid (top row), a high acidity of the thorium solution (middle row), and a low concentration of the thorium solution (bottom row), scalebars 2 μm (left) and 10 μm (right) side, micrographs from **publication II**.*

Follow-up research in **publication IV** examined the homogeneous hydrolysis of Ce(III and IV), Nd(III), UO_2^{2+} , and their mixtures. The uranyl ion hydrolysed at $\text{pH} = 4.5$ to ammonium diuranate of different stoichiometry depending on the experimental parameters. Ce(IV) was prone to hydrolysis and gave nanocrystalline CeO_2 already at $\text{pH} = 1.3$. Ce(III), on the other hand, started to precipitate at $\text{pH} = 5.2$, similar to Nd(III). Complex binary and ternary ion mixtures were hydrolysed as well with the aim of testing the procedure for the preparation of

minor actinide-bearing transmutation fuel.

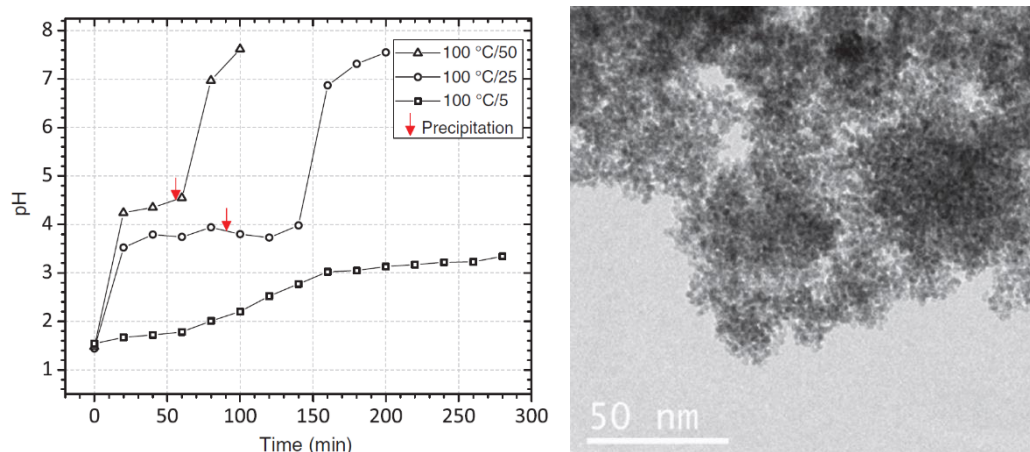


Figure 8 Kinetics of homogeneous hydrolysis of thorium nitrate solution by decomposition of urea (left), final nanocrystalline ThO₂ product by electron microscopy (right, from **publication III**).

On top of that, non-conventional uranium carbide (fast reactor fuel) synthesis was developed, and the details are discussed in **publication V**. Previously, uranium carbide has been mainly prepared by carbothermal reduction of UO₂ using graphite at 1600 °C⁶¹. It was found that a mixture of uranyl nitrate and citric acid gives at 800 °C under inert conditions a nanocomposite of UO₂ nanocrystals embedded in an active carbon matrix, see Figure 9 (left). This nanocomposite possesses an extensive interphase area between the UO₂ crystallites and active carbon, naturally much more prominent than after mixing and blending graphite and UO₂ powder. Good powder mixing increases the homogeneity and reaction interphase and is essential for efficient carbothermal reduction. Indeed, the UC formation occurred already at 1200 °C on a minute timescale (Figure 9 right) compared to conventional hours at 1600 °C. The sintering behaviour of the UC powder prepared using this technique is described later in **publication XIX**.

2.2 Oxalate derived ThO₂ powder and its sintering performance

Even though the oxalate-derived ThO₂ was a subject of various sintering studies in the past^{62,63},

⁶¹ R.B. Matthews, R.J. Herbst: Uranium-plutonium carbide fuel for fast breeder reactors, Nuclear Technology 63 (1983) 9-22.

⁶² Y. Harada, Y. Baskin, J.H. Handwerk: Calcination and sintering study of thoria, Journal of the American Ceramic Society 45 (1962) 253-257.

⁶³ J.M. Pope, K.C. Radford: Physical-properties of some thoria powders and their influence on sinterability, Journal of Nuclear Materials 52 (1974) 241-254.

⁶⁴, a complex study describing the synthesis, calcination, and sintering needed to be included. **Publication VI** introduced a comprehensive study of the precipitation and calcination parameters of binder-less sintering of oxalate-derived ThO₂ powders. The preparation of mechanically stable high-density pellets was found to be a complex problem when precipitation strike affected the powder postproduction, packing density, etc.

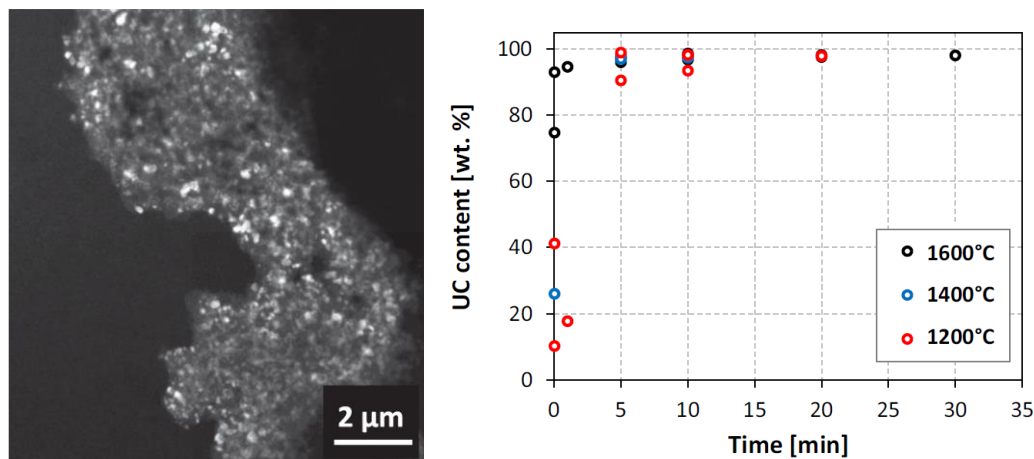


Figure 9 Transmission electron microscopy of the uranyl nitrate/citric acid solution dried and treated at 1000 °C under inert conditions forming UO₂/C composite, kinetics of carbothermal reduction of the UO₂/C nanocomposite at different temperatures (from **publication V**).

Powder fired at higher temperatures gave better green density but densified less. Important CO₂ adsorption was also identified for powders calcined at low (600 °C) temperatures. After all, pellets with >90% density at 1625 °C and >98% at 1750 °C were obtained. These pellets would meet the specifications to be used, for example, in CANDU reactors.

The platelet morphology of ex-oxalate agglomerates is generally considered a disadvantage of oxalate derive oxide powders due to low packing density (green density). Theoretically, the best grain morphology for packing and sintering is a sphere. However, a spherical morphology would require a milling step, which is problematic for industry from the viewpoint of airborne radioactive dust contamination.

Thus, the approaches in **publication II** (thorium oxalate morphotypes) and **VI** (conventional sintering of oxalate derived ThO₂) were combined and resulted in **publication VII**. The link between the oxalate shape and the sintering performance of the derived ThO₂ was examined ex-situ by pressing, sintering, and dilatometry. Figure 10 shows the different morphotypes

⁶⁴ G.D. White, L.A. Bray, P.E. Hart: Optimization of thorium oxalate precipitation conditions relative to derived oxide sinterability, Journal of Nuclear Materials 96 (1981) 305-313.

prepared on a large scale (gram amounts), converted to oxide at 700 °C (3 hours), and their sintering performance by dilatometric measurements. The best ex-situ sintering performance showed powder #1 (Figure 10), which was prepared at a low temperature (5 °C). Although it had a lower packing density, the shrinkage at 1625 °C was about 30% showing a final density of 75%, all other powders gave pellets below 70%. An important fact was that the presence of a hole inside the ex-oxalate ThO_2 agglomerate increased the final density. Additionally, it was observed that pellets produced from oxalates with large platelets tend preferentially stack during pressing.

2.3 Application of oxalate derived oxide powders/pellets

The knowledge of ThO_2 and UO_2 powder synthesis and sintering allows to produce samples, which can be further used for unique measurements or as reactants in consequent synthesis. In **publication VIII**, the oxalate derived ThO_2 powder was successfully sintered into high-density pellets, which were used later for the measurement of basic physical properties.

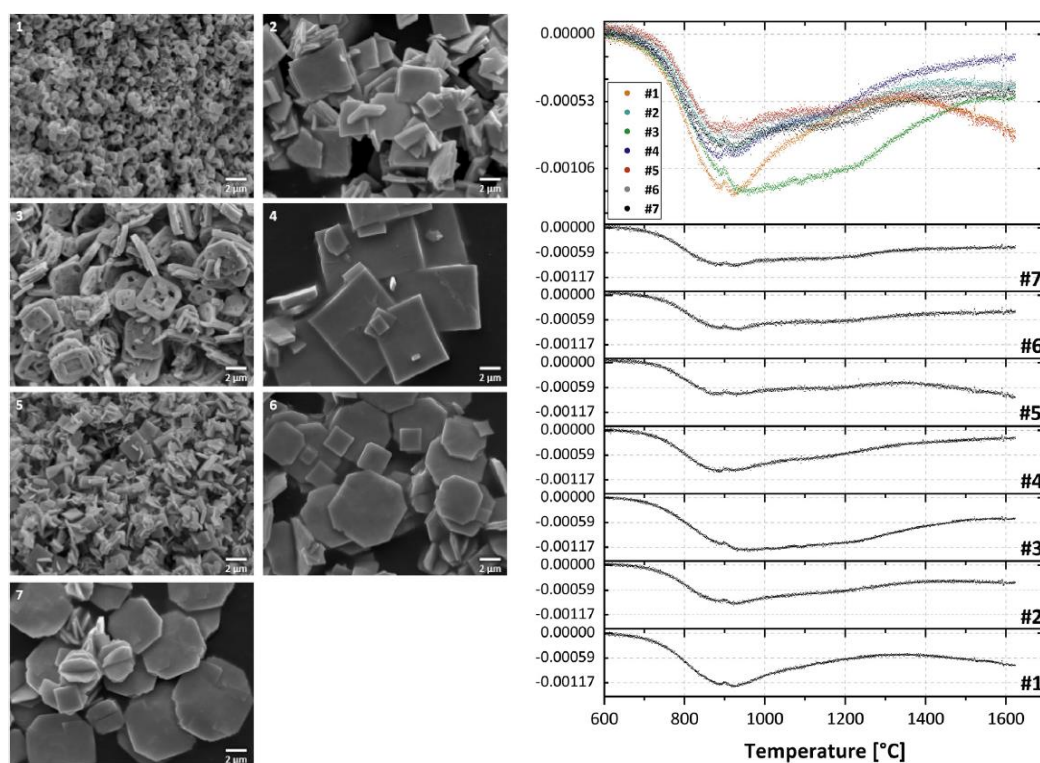


Figure 10 Different morphotypes of oxalate derived ThO_2 and their sintering performance by dilatometry (from **publication VII**).

Measurements of thermal conductivity, specific heat, and thermal diffusivity, the spectral and total hemispherical emissivity of ThO_2 were shown and discussed in the temperature range

2000 K to 3050 K. Additionally, the melting point of ThO_2 was redetermined to be 3665 ± 70 K. Examples of the physical properties measured in work are shown in Figure 11, e.g., the plot of thermal conductivity (left) and specific heat capacity (right).

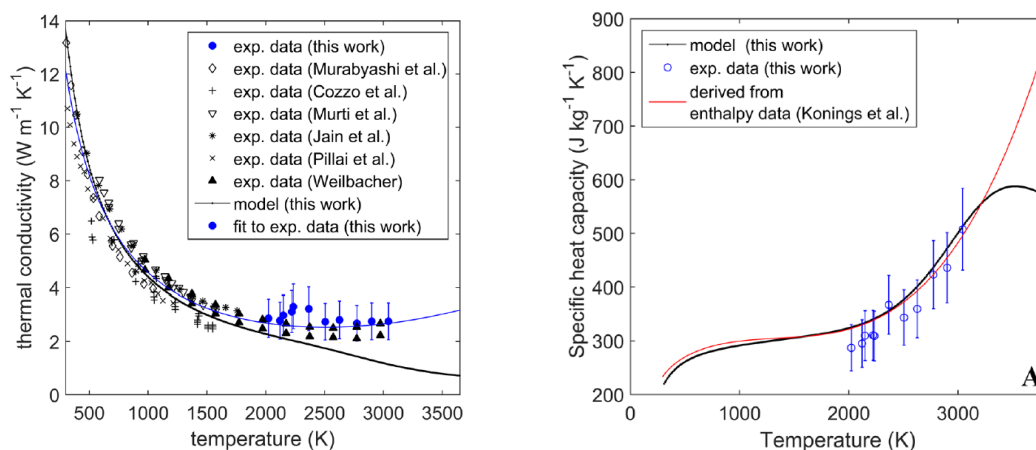


Figure 11 Measurements of thermal conductivity (left) and specific heat capacity of ThO_2 in the range 2000-3050 K (from **publication VIII**).

The thermodynamic properties of materials are of extreme importance in nuclear technology. Heat and consequent electricity generation carry specific phenomena that must be considered for nuclear fuel such as safety margin to melting linked to the heat capacity and conductivity, high-temperature creep, radiation tolerance, recrystallization etc. Another philosophy must be accepted when considering a nuclear reactor using molten salts as fuel (Gen IV concept). Apart from the nuclear properties (neutronics), the molten fuel must fulfil specific physicochemical criteria like melting behaviour, actinide solubility in the fuel matrix, density, viscosity, etc. One main direction in the molten salt reactor concept is based on fluorides⁶⁵. Oxalate-derived oxides can contribute to this research as synthetic precursors for UF_4 and ThF_4 , see **publication VIII**. One advantage of using uranium and thorium oxalates is that after conversion to oxides at lower temperatures (500-800 °C), they yield porous powders with high specific surface area. This is convenient for the solid/gas reaction when transforming oxide to fluoride by reaction with gaseous HF. The purity of the fluoride compounds was controlled by the determination of the melting points. Especially in the case of uranium presence of higher oxidation states (V, VI) can cause a significant shift of the melting point towards lower temperatures. The melting point of UF_4 was, in this case, measured for the first time by a direct

⁶⁵ O. Beneš, R.J.M. Konings: Molten salt reactor fuel and coolant, chapter 3.13 in *Comprehensive Nuclear Materials*, Elsevier, 2012.

calorimetric technique (1034.7 ± 3 °C).

2.4 Scrap recycling in ThO₂ pellets production

As mentioned in the introduction, every chemical technology has to minimize its waste production and, if possible, reuse its reagents in the form of a technological loop. Conventional UO₂ fuel production reuses oxidized pellet scrap as a sintering additive in the primary powder blend and therefore has no waste. This is, however, not possible in the case of ThO₂, which does not have higher valence oxides promoting sintering. Thus, the recycling of ThO₂ pellet scrap must be fundamentally different, most probably through the solution chemistry approach. The existing THOREX (thorium uranium extraction) approach uses a mixture of HNO₃, HF (catalytic amount), and Al(NO₃)₃ (anticorrosion agent)^{66,67} to dissolve ThO₂. Such composition of the digestion solution brings problems with corrosion, undesired precipitation of ThF₄, and Al contamination. The ThO₂ pellet scrap recycling route based on triflic acid dissolution and thorium separation by oxalic precipitation was demonstrated for the first time in **publication X** and extended in **publication XI**. The recycling loop is visualized in Figure 12 with arrows showing processing directions, entering chemicals, and main components.

It was demonstrated that triflic acid could effectively dissolve dense ThO₂, the main disadvantage is the slower kinetics than the THOREX mixture. However, one should consider that no catalyst (like HF) is present. Thorium (IV) ions can be separated and precipitated from the solution as thorium oxalate, which serves as a precursor for oxide to be introduced again in the fuel production cycle.

Publication XI described the solution acidity's effect on the oxalate's precipitation yield. It was found that triflic acid positively affects the yield compared to nitric acid in which the loss of Th is more significant. The reason is that triflic acid does not form soluble complexes with thorium in highly concentrated solutions, which is the case for nitric acid. Additionally, the coprecipitation of Ra (II) was studied as a function of the solution acidity. An interesting observation was that in a highly concentrated triflic acid solution (hygroscopic), Th(C₂O₄)₂·2H₂O was formed instead of typical Th(C₂O₄)₂·6H₂O. In conclusion, it was demonstrated that the recycling loop using triflic acid and oxalic precipitation is a viable proof

⁶⁶ D. Das, S.R. Bharadwaj: Thorium-based Nuclear Fuels, 1st Edn. Springer, London, 2013.

⁶⁷ W.D. Bond: Dissolution of sintered thorium-uranium oxide fuel in nitric acid-fluoride solutions. Report ORNL-2519, Oak Ridge National Laboratory, Oak Ridge, 1958.

of concept that could be tested on a large scale.

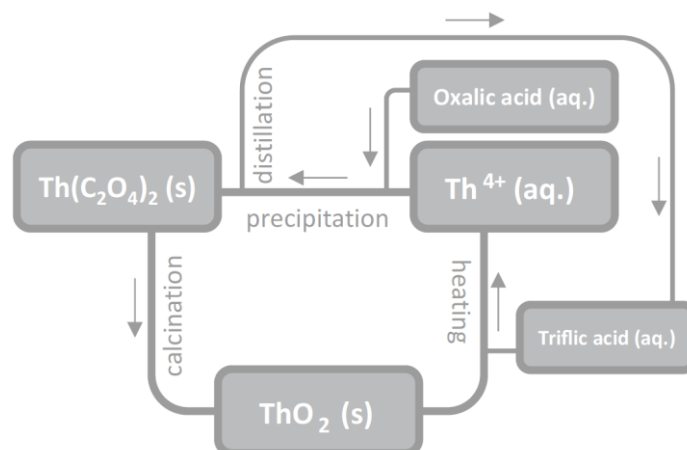


Figure 12 A closed loop of the ThO_2 recycling process based on triflic acid dissolution (right), oxalate precipitation (top), conversion to oxide (left), and the recovery of triflic acid by distillation (from **publication XI**).

2.5 Spark plasma sintering of UO_2 , ThO_2 , UC powders

Handling radioactive powders requires decent working conditions and specific measures. These aspects are covered by radioprotection, a field of workplace safety in controlled areas with possible radioactive contamination. Concerning radioactive substances, two phenomena are possible: i) Exposure to ionizing radiation, ii) Contamination, which can be external or internal. The heart of radiation safety is the “ALARA” principle (As Low As Reasonably Achievable)⁶⁸, which instructs the personnel to keep the radiation dose to a human body as low as reasonably possible. Therefore, when considering to instal a spark plasma sintering facility at JRC Karlsruhe, it was crucial to adopt the whole apparatus for radiotoxic materials according to the principles of radiation safety. **Publication XII** describes the successful efforts in the integration of a modified SPS facility (FCT Systeme GmbH, Rauenstein, Germany) into a hermetic glovebox, see Figure 13. It was proven that the integration had no negative effect on the performance of the facility, and the first SPS sintering of UO_{2+x} powder was conducted. After some adjustments and testing UO_2 pellet of 97% density was successfully prepared within 5 minutes at 1000 °C. One can say that the initial stage of mastering UO_2 powder SPS sintering was accomplished, and dense bodies could be prepared without complications.

As mentioned earlier, ThO_2 is more difficult to sinter to high density than UO_2 . So, the

⁶⁸ International Atomic Energy Agency: IAEA Safety Glossary, Terminology Used in Nuclear Safety and Radiation Protection, Vienna, 2007.

consequent challenges in SPS activities were obvious. In **publication XIII**, the oxalate-derived ThO₂ powders with different average crystallite sizes (13, 19, and 34 nm) were examined in a SPS sintering study and compared to a commercial powder. It was found that the sintering behaviour of the oxalate-derived powders can be split into two stages, the first stage is linked to the initial grain size (calcination temperature), and the second takes place at a similar temperature for all the powders. The first sintering stage concerns grain growth and sintering within the ex-oxalate grains, while the second stage concerns the necking/sintering between the ex-oxalate grains. In general, SPS proved to be an efficient tool for the preparation of dense ThO₂ compacts (>95%). The main disadvantage was that pellets were more brittle than conventionally sintered. This can be explained by the reducing environment in SPS since the hardness (also brittleness) of ThO₂ is higher for the sample obtained at reducing conditions⁶⁹.

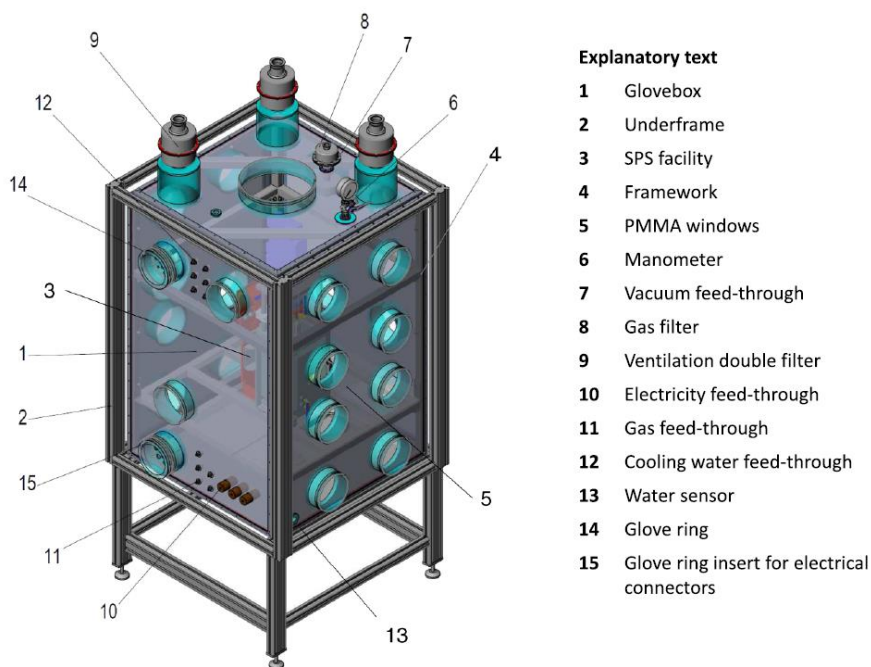


*Figure 13 Representation of SPS facility integrated to a hermetic glovebox to handle radiotoxic materials (from **publication XII**).*

Attention was also given to the separate effect studies concerning spent nuclear fuel. This concern is mainly spent on surrogate fuel manufacturing. **Publication XIV** described the preparation and characterisation of UO₂/CsI high-density composite pellets, which has not been reported before. Cs and I are essential fission products present in spent fuel, therefore

⁶⁹ A. Baena, T. Cardinaels, J. Van Eyken, J.L. Puzzolante, K. Binnenmans, M. Verwerft: Effect of sintering atmosphere on the hardness of ThO₂, Journal of Nuclear Materials 477 (2016) 222-227.

significant attention is given to their behaviour, especially accidental release⁷⁰. By lowering the sintering temperature of UO_2 to $1000\text{ }^\circ\text{C}$, it was possible to embed and encapsulate CsI in closed porosities. The boiling point of CsI is $1280\text{ }^\circ\text{C}$, thus the sintering temperature is far below this point, and the salt did not vaporise. The application of SPS was essential to achieve these results since conventional sintering requires temperatures $> 1600\text{ }^\circ\text{C}$. The relevancy of these results was supported by a selection of our contribution for the cover picture of Journal of Nuclear Materials Volume 466 (Figure 14). Apart from fission product studies in spent fuel, the fuel restructuring at the pellet periphery (high burn-up structure, HBS) was in the research spotlight. The fuel undergoes important microstructural changes during the lifetime in the reactor core, and one of the main features is the decrease of the grain size in HBS from several micrometres to tens of nanometres⁷¹. Therefore, preparing dense fuel pellets with nanometric grain size was another goal of the SPS sintering studies.

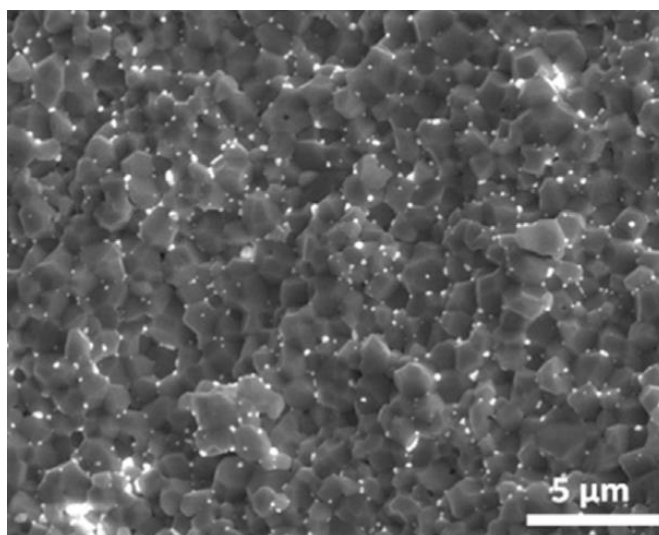


Figure 14 Fracture surface of 1 mol% doped CsI- UO_2 from as received UO_2 by scanning electron microscopy (from **publication XIV**).

UO_{2+x} powders prepared by gel-supported precipitation were SPS compacted with the aim of receiving dense pellets ($> 90\%$) and the lowest grain size (**publication XV**). With applied pressure of 100 MPa and fast quenching from the desired temperature, the average grain size as small as 300 nm was achieved without using any special treatment or tooling. Naturally, smaller gain sizes presented a challenge in the following research. The high-pressure variant

⁷⁰ I. Johnson, C.E. Johnson: Mass spectrometry studies of fission product behavior. I. Fission products released from irradiated LWR fuel, Journal of Nuclear Materials 154 (1988) 67-73.

⁷¹ H.J. Matzke, J. Spino: Formation of the rim structure in high burnup fuel, Journal of Nuclear Materials 248 (1997) 170-179.

of SPS was applied to consolidate nanometric oxalate-derived UO_2 powders in **publication XVI**. Silicon carbide punches were used to sinter powders instead of graphite punches⁷², allowing application pressure of up to 500 MPa. The high-pressure setup is depicted in Figure 15. The UO_2 nanocrystalline powder with an average grain size of 11 nm was sintered using HPSPS to densities > 80% while maintaining the grain size below 60 nm. In both presented works on small grain pellets, the SPS process was terminated at the desired temperature, and the whole die/punch system with the pellet was quenched as fast as possible to room temperature. This process of time control and fast cooling allowed us to reduce grain growth and achieve the best possible results.

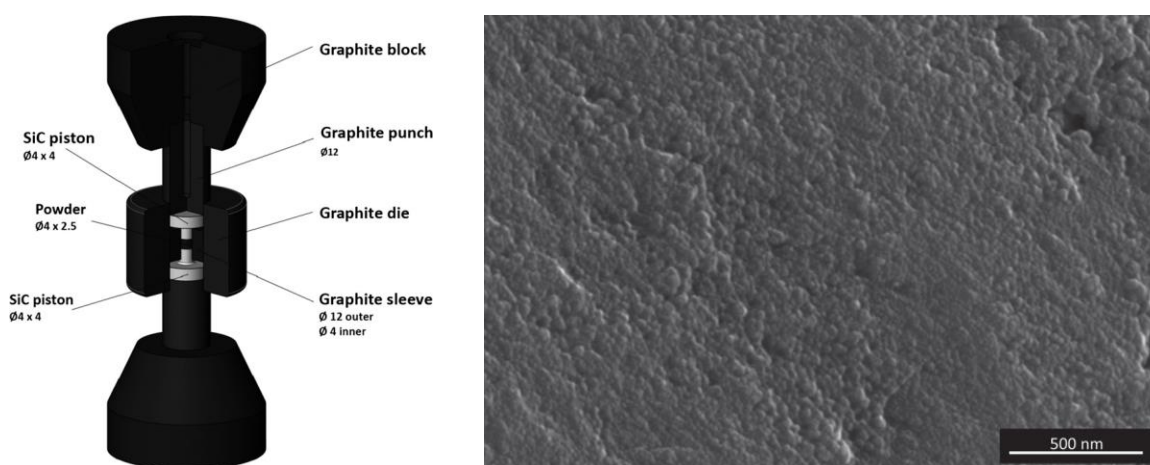


Figure 15 High-pressure SPS setup with SiC punches able to reach 500 MPa (left), scanning electron micrographs of the pellet fresh fracture surface for sample quenched from 835 °C (from **publication XVI**).

During the studies, the basic phenomena of FAST technology were also touched on. **Publication XVII** explored the role of the electrical in spark plasma sintering of UO_{2+x} . It was found that the sintered UO_{2+x} pellets had a gradient in grain size and in oxygen stoichiometry linked with the electrical polarity of the graphite punches. The gradient of the oxygen content was caused by two superimposing effects: i) the reducing effect of the graphite environment and (ii) the direction of the electrical field, which attracts oxygen anions toward the anode punch. These effects were saved into the pellet microstructure, at first, the oxygen stoichiometry (O/U molar ratio) decreased from the edge close to the anode to the cathode, which is connected with defect distribution. This is associated with the cationic diffusivity, which is larger for U (V) and U (VI) in the oxygen-rich region, and therefore the grain growth

⁷² U. Anselmi-Tamburini, J.E. Garay, Z.A. Munir: Fast Low-Temperature consolidation of bulk nanometric ceramic materials, *Scripta Materialia* 54 (2006) 823–828.

is more significant in that region, see Figure 16. Thus, one can say that SPS sintering of UO_{2+x} is more complex than simple ceramics like Al_2O_3 ⁷³, and the electrical field effects must be considered.

Lastly, as a continuation of **publication V** in section 2.1, the UC powder was processed in SPS to prepare high-density fuel pellets, as described in **publication XVIII**. The synthesis, presented in **publication V.**, yielded very fine and sinter-active powder, thus a successful SPS sintering study was conducted. Three different powders (obtained at 1200, 1400, and 1600 °C) were sintered at 1700 °C for 10 minutes and 100 MPa of applied pressure. The sintering onset was linked with the preparation temperature, while the finest powder (1200 °C) showed the highest compaction and yielded pellets with 95 % density. An interesting observation was a partial decomposition of UC. The original powder (1200 °C) contained about 3 wt.% of UO_2 contamination (by pXRD), after sintering, the sample had 7 wt.% of UO_2 and, surprisingly 8 wt.% of UC_2 phase. However, even for carbide fuel, the FAST techniques proved their efficiency in the production of high-density compacts at milder conditions than conventional sintering.

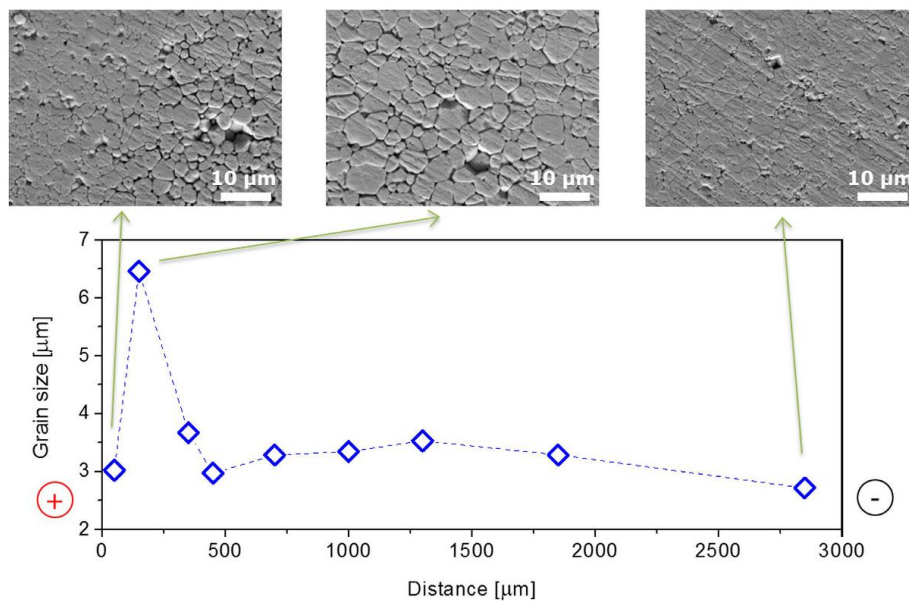


Figure 16 The grain size distribution of UO_{2+x} pellet after SPS sintering at 1200 C for 5 minutes, measured in the centre of the pellet (from **publication XVII**).

⁷³ U. Anselmi-Tamburini, S. Gennari, J.E. Garay, Z.A. Munir: Fundamental investigations on the spark plasma sintering/synthesis process: II. Modeling of current and temperature distributions, Materials Science and Engineering A 394 (2005) 139-148.

3 Conclusion

The nuclear energy sector has gone through seventy years of development. Since the early days, it has been heavily affected by political and societal aspects. Therefore, the investments in constructing new power plants and research budgets have come in irregular waves and were strongly hit by the Chernobyl and Fukushima accidents. However, since 1970th, the nuclear industry has been a reliable and stable energy source with all its negative and positive aspects. The presented habilitation thesis summarized the research of 18 publications carried out in the field of powder synthesis and processing related to the nuclear fuel cycle. Synthetic and processing techniques are generally new and mainly not applied in the industrial nuclear fuel cycle. However, they have industrialisation potential since most of the research presented was designed with a considerable focus on applicability.

Except for plutonium oxalate, which is already used in the industry, new results on the synthesis of actinide (U, Th) oxalates, their thermal conversion to oxides, and sintering behaviour were discussed. It was shown that oxalate precipitation is an efficient, robust, and low-cost synthetic route but precise enough to control the morphology, grain size, and other parameters of the final product important for powder metallurgy. Homogeneous precipitation using urea decomposition was tested on uranium, thorium, and selected lanthanides. In the case of Th (IV) the synthesis yielded fine oxide nanoparticles with coprecipitated Ra(II). Apart from ceramic compacts production, it was shown that oxalate-converted powders could serve as reactants for the next synthetic steps or starting material for the production of bodies with quality enabling measurements of special physical properties. A new technological loop of the ThO₂ scrap recycling was established using triflic acid dissolution and oxalic precipitation. A different aspect of this process was discussed, considering the efficiency, radium coprecipitation, and product properties. The nonconventional synthesis and sintering of generation IV carbide fuels were touched as well, both the preparation and SPS sintering proved their enormous efficiency compared to the classic powder metallurgy approach, saving time and energy, especially in research fuel production.

The electrical field sintering techniques certainly have become important in the technology of refractory ceramics, metals, and alloys. In the past ten years, especially spark plasma sintering found its confirmed place in the preparation of nuclear fuel for research purposes. By

positively affecting the sintering conditions of refractory materials, the SPS technology allowed to compact of UO_2 , ThO_2 , and UC at significantly milder conditions than the classical sintering process. Moreover, it facilitated the preparation of entirely new materials. The presented thesis showed successful compaction of UO_2 pellets with grain sizes below 500 nm with SPS or even below 100 nm using high-pressure SPS. Further, UO_2/CsI composite fuel pellets were produced for the first time. Both materials are suitable for separate effect studies on spent nuclear fuel, which are not possible with the real material due to its high radioactivity and complex behaviour. One of the critical questions in the FAST basic research considers the fundamental electrical field effects (athermal) on compaction, grain growth, final microstructure, etc. The attractive gradient in the microstructure and oxygen content was observed in the SPS-sintered UO_{2+x} . Since the sintering activity relates to the O/U stoichiometry and consequently with the oxidation state of uranium, the atypical microstructure could be explained and contributed to the mechanism of FAST sintering of oxygen conductive fluorites.

The results presented in the thesis seeded several new research topics, which are currently under investigation at various institutes and Charles University. The homogeneous precipitation techniques are developed in collaboration with SCK·CEN, Belgium, where the main focus is given to the growth of thorium oxalate. At Charles University, this technique is applied to lanthanide oxalates, the development of single crystals, and structure determination. In the field of FAST techniques, several research lines exist at the moment. New high-pressure SPS experiments and simulations are conducted in collaboration with KU Leuven, Belgium. Basic phenomena describing the grain growth of CeO_2 in AC/DC electrical fields are investigated in collaboration with JRC Karlsruhe, Germany.

4 List of publications

Publications considered for this habilitation thesis ordered into topical groups:

UO₂, ThO₂, UC, doped UO₂ powder preparation (section 2.1)

- I. **V. Tyrpekl**, J-F. Vigier, D. Manara, T. Wiss, O. Dieste Blanco, J Somers: Low temperature decomposition of U(IV) and Th(IV) oxalates to nanograined oxide powders (2015) *Journal of Nuclear Materials*, 460, pp. 200-208.
- II. **V. Tyrpekl**, M. Beliš, T. Wangle, J. Vleugels, M. Verwerft: Alterations of thorium oxalate morphology by changing elementary precipitation conditions (2017) *Journal of Nuclear Materials*, 493, pp. 255-263.
- III. T. Wangle, **V. Tyrpekl**, T. Delloye, O. Larcher, J. Pakarinen, T. Cardinaels, J. Vleugels, M. Verwerft: Homogeneous hydrolysis of thorium by thermal decomposition of urea (2018) *Radiochimica Acta*, 106 (8), pp. 645 – 653.
- IV. C. Schreinemachers, O. Bollen, G. Leinders, **V. Tyrpekl**, G. Modolo, M. Verwerft, K. Binnemans, T. Cardinaels: Hydrolysis of Uranyl-, Nd-, Ce-Ions and their Mixtures by Thermal Decomposition of Urea (2022) *European Journal of Inorganic Chemistry*, 2022 (4), art. no. e202100453.
- V. D. Salvato, J-F. Vigier, O. Dieste Blanco, L. Martel, L. Luzzi, J. Somers, **V. Tyrpekl**: Innovative preparation route for uranium carbide using citric acid as a carbon source (2016) *Ceramics International*, 42 (15), pp. 16710-16717

Oxalate derived ThO₂ powder and its sintering performance (section 2.2)

- VI. T. Wangle, **V. Tyrpekl**, S. Cagno, T. Delloye, O. Larcher, T. Cardinaels, J. Vleugels, M. Verwerft: The effect of precipitation and calcination parameters on oxalate derived ThO₂ pellets (2017) *Journal of Nuclear Materials*, 495, pp. 128-137.
- VII. T. Wangle, M. Beliš, **V. Tyrpekl**, J. Pakarinen, T. Cardinaels, T. Delloye, J. Vleugels, M. Verwerft: Morphology dependent sintering path of nanocrystalline ThO₂ (2020) *Journal of Nuclear Materials*, 533, art. no. 152081.

Application of oxalate derived oxide powders/pellets (section 2.3)

- VIII. T.R. Pavlov, T. Wangle, M.R. Wenman, **V. Tyrpekl**, L. Vlahovic, D. Robba, P. Van Uffelen, R.J.M. Konings, R.W. Grimes: High temperature measurements and condensed matter analysis of the thermo-physical properties of ThO₂ (2018) *Scientific Reports*, 8 (1), art. no. 5038.
- IX. P. Souček, O. Beneš, B. Claux, E. Capelli, M. Ougier, **V. Tyrpekl**, J-F. Vigier, R.J.M. Konings:

Synthesis of UF₄ and ThF₄ by HF gas fluorination and re-determination of the UF₄ melting point (2017) *Journal of Fluorine Chemistry*, 200, pp. 33-40.

Scrap recycling in ThO₂ pellets production (section 2.4)

- X. S. Cagno, L. Gijsemans, **V. Tyrpekl**, T. Cardinaels, M. Verwerft, K. Binnemans: Use of triflic acid in the recycling of thoria from nuclear fuel production scrap (2017) *Journal of Sustainable Metallurgy*, 3 (3), pp. 659-667.
- XI. **V. Tyrpekl**, R. Lommelen, T. Wangle, T. Cardinaels, K. Binnemans, J. Vleugels, M. Verwerft: Studies on the Thoria Fuel Recycling Loop Using Triflic Acid: Effects of Powder Characteristics, Solution Acidity, and Radium Behavior (2019) *Journal of Sustainable Metallurgy*, 5 (1), pp. 118-126.

Spark plasma sintering of UO₂, ThO₂, UC powders (section 2.5)

- XII. **V. Tyrpekl**, C. Berkmann, M. Holzhäuser, F. Köpp, M. Cologna, T. Wangle, J. Somers: Implementation of a spark plasma sintering facility in a hermetic glovebox for compaction of toxic, radiotoxic, and air sensitive materials (2015) *Review of Scientific Instruments*, 86 (2), art. no. 023904.
- XIII. **V. Tyrpekl**, M. Cologna, D. Robba, J. Somers: Sintering behaviour of nanocrystalline ThO₂ powder using spark plasma sintering (2016) *Journal of the European Ceramic Society*, 36 (3), pp. 767-772.
- XIV. T. Wangle, **V. Tyrpekl**, M. Cologna, J. Somers: Simulated UO₂ fuel containing CsI by spark plasma sintering (2015) *Journal of Nuclear Materials*, 466, pp. 150-153.
- XV. M. Cologna, **V. Tyrpekl**, M. Ernstberger, S. Stohr, J. Somers: Sub-micrometre grained UO₂ pellets consolidated from sol gel beads using spark plasma sintering (SPS) (2016) *Ceramics International*, 42 (6), pp. 6619-6623.
- XVI. **V. Tyrpekl**, M. Cologna, J-F. Vigier, A. Cambriani, W. De Weerd, J. Somers: Preparation of bulk-nanostructured UO₂ pellets using high-pressure spark plasma sintering for LWR fuel safety assessment (2017) *Journal of the American Ceramic Society*, 100 (4), pp. 1269-1274.
- XVII. **V. Tyrpekl**, M. Najj, M. Holzhäuser, D. Freis, D. Prieur, P.M. Martin, B. Cremer, M. Murray-Farthing, M. Cologna: On the Role of the Electrical Field in Spark Plasma Sintering of UO_{2+x} (2017) *Scientific Reports*, 7, art. no. 46625.
- XVIII. D. Salvato, J-F. Vigier, M. Cologna, L. Luzzi, J. Somers, **V. Tyrpekl**: Spark plasma sintering of fine uranium carbide powder (2017) *Ceramics International*, 43 (1), pp. 866-869.